

Synthetic diamond and wurtzite structures self-assemble with isotropic pair interactions

Mikael C. Rechtsman,¹ Frank H. Stillinger,² and Salvatore Torquato^{2,3,4}

¹*Department of Physics, Princeton University, Princeton, New Jersey, 08544, USA*

²*Department of Chemistry, Princeton University, Princeton, New Jersey, 08544, USA*

³*Program in Applied and Computational Mathematics and PRISM, Princeton, New Jersey, 08544, USA*

⁴*Princeton Center for Theoretical Physics, Princeton, New Jersey, 08544, USA*

(Received 23 September 2006; revised manuscript received 11 January 2007; published 26 March 2007)

Using inverse statistical-mechanical optimization techniques, we have discovered isotropic pair interaction potentials with strongly repulsive cores that cause the tetrahedrally coordinated diamond and wurtzite lattices to stabilize, as evidenced by lattice sums, phonon spectra, positive-energy defects, and self-assembly in classical molecular dynamics simulations. These results challenge conventional thinking that such open lattices can only be created via directional covalent interactions observed in nature. Thus, our discovery adds to fundamental understanding of the nature of the solid state by showing that isotropic interactions enable the self-assembly of open crystal structures with a broader range of coordination number than previously thought. Our work is important technologically because of its direct relevance generally to the science of self-assembly and specifically to photonic crystal fabrication.

DOI: [10.1103/PhysRevE.75.031403](https://doi.org/10.1103/PhysRevE.75.031403)

PACS number(s): 82.70.Dd, 81.16.Dn

I. INTRODUCTION

The science of “self-assembly,” as introduced by Whitesides and co-workers about 15 years ago [1] as a promising research direction, is a large and rapidly growing field of tremendous technological potential and fundamental interest. Its motivating factor is simple: direct micro- and nanofabrication of circuitry (electronic, optoelectronic, or others) becomes prohibitively time consuming and/or expensive below a certain length scale, and, as a result, scientists and engineers are searching for particles on the mesoscopic scale that by themselves assemble into potentially useful structures by virtue of their mutual interactions; hence the term self-assembly. There is a large number of examples of theoretical, experimental, and computational studies on this topic [2–6]. Colloidal systems command particular interest, as interaction potentials in these systems have become increasingly tailorable with the advent of new ways to functionalize the colloidal surface. These systems have tremendous capacity to assemble exotic lattices and hence to yield photonic band gap structures. In particular, the diamond lattice is known to have a pronounced photonic band gap [7].

In this paper, we obtain the fundamentally and technologically important result that the three-dimensional diamond and wurtzite structures can self-assemble with isotropic interactions possessing a strongly repulsive core, and present the corresponding potential functions, which have been derived using optimization techniques developed previously [8]. Specifically, we show that an N -body classical system with particles interacting via one of our derived isotropic potentials has as its ground state the corresponding lattice, in a specific volume (or density) range. Unlike previous attempts to solve this problem, we come to this conclusion only after satisfying several important criteria: (1) lattice sums show that there is a positive pressure range in which the given lattice is stable; (2) all crystal normal mode frequencies are real at specific volume v ; (3) defects (vacancies and interstitials) are shown to cost the system energy; and (4)

the system self-assembles in a molecular dynamics simulation that starts above the freezing point and is slowly cooled. In (4), the system may start from an entirely random configuration or with a layer of fixed particles to promote epitaxial growth. Hence we make the important distinction here between homogeneous and heterogeneous nucleation in self-assembly. It is of course a more stringent requirement that the desired lattice self-assemble from a random configuration (homogeneous). We find that the diamond crystal assembles from a completely random configuration, but the wurtzite crystal requires an epitaxial layer for it to do so (heterogeneous).

The importance of criterion (4) to establish a ground state structure has been generally overlooked in previous work. Currently, most studies rely exclusively on criteria (1) and/or (2) to determine lattice stability. The only result that is guaranteed by satisfying (1) and (2) is that the structure is a local minimum, not a global one. Computationally, the only practical way that one can ensure that the desired target structure is the ground state is by doing the cooling and annealing step (4). However, if the presumed ground state is not achieved by an annealing, it does not necessarily imply that it is not the ground state if the resulting energy of the structure produced exceeds that of the target structure. There may simply be a kinetic bottleneck that prevents the annealing process from finding the ground state in a reasonable amount of computer time.

The approach by theorists and experimentalists toward finding complex self-assembling materials has primarily been *Edisonian* (i.e., trial and error) in nature rather than being systematic and deductive. Motivated by the increasing control that experimentalists have over interparticle interactions, in colloids in particular, we have previously derived a systematic procedure to optimize these interactions to produce desired structures. This is an example of “inverse statistical mechanics.” Instead of using the interactions in a system to find the resulting behavior, we target a particular behavior (e.g., structure), and derive optimal interactions to yield such a result. We have recently applied these schemes

to two-dimensional monodisperse, isotropic systems [8], and in the present paper, we use one of these methods, the so-called zero-temperature scheme, to derive isotropic interaction potentials that permit the self-assembly of the diamond and wurtzite lattices, respectively. The self-assembly of any low-coordinated target structure in three dimensions is considerably more challenging than in two dimensions because the number of possible competing structures grows dramatically with increasing dimension.

With the exception of the so-called patchy particles [9], colloidal interactions are isotropic, and thus we believe it is a technologically relevant as well as theoretically intriguing question to ask: What are the limits of isotropic interaction potentials for self-assembly? Our discovery adds to fundamental understanding of the nature of the solid state by showing that isotropic interactions enable the self-assembly of crystal structures with a much broader range of coordination numbers than previously thought.

The self-assembly of a diamond lattice of dielectric spheres has been something of an ultimate goal in colloid science, since it was found that in the diamond lattice, unlike in the face-centered cubic (fcc) and body-centered cubic (bcc) lattices, for example, there exists a band gap in the photonic spectrum [7]. This is the central necessary condition for and enabler of photonic circuitry, since this property allows control over passage vs blockage of light, in analogy to the way transistors control electric current [10]. It should be noted that there has been recent work on icosahedral quasicrystals as desirable photonic band gap structures [11]. While this is a promising avenue of research, its central stumbling block is that self-assembly of quasicrystals in three dimensions is extremely difficult. Indeed, a single defect destroys strict quasicrystallinity. Furthermore, there is an ongoing controversy over whether a quasicrystal can be assembled using only local information. The diamond-structure potential we find is radially complex, and seemingly difficult to fabricate in the laboratory directly. That said, technology that allows experimentalists to control colloidal and nanoparticle interaction has been advancing significantly in recent years, with DNA functionalization [3], for example, becoming a very useful method. Furthermore, radial complexity in the interaction potential is found in potentials of mean force [12]. Recently, experimentalists have observed diamondlike behavior in mixed silver and gold nanoparticle systems [13]; however, the precise form of the interparticle interaction potential is currently unknown.

Watzlawek, Likos, and Löwen (WLL) have devised an isotropic interaction potential that models star polymer systems, with good agreement with experiment [14]. In particular, WLL have found, for certain of their parameters, a region of stability for the diamond lattice, and thus an isotropic potential that favors it. The type of potential used in the WLL study has a soft core; in particular, for small r , $V(r) \sim -\log(r)$. While their potential is structurally simpler than the one we present here, it is not a potential that can be considered analogous to those in colloidal systems with present technology because colloidal particles have too hard a core. We have discovered, in the course of performing optimization runs, that assembling open lattices with hard core potentials requires the potential to have more features than that of the WLL potential.

TABLE I. Coordination structure of the diamond and wurtzite lattices. Here, we set a to be the distance to the nearest neighbor. If both lattices have the same specific volume, a for diamond is equal to a for wurtzite.

r/a	Diamond	Wurtzite
1	4	4
$\sqrt{8/3}$	12	12
$5/3$	0	1
$\sqrt{11/3}$	12	9
$\sqrt{16/3}$	6	6
$7/3$	0	6
$\sqrt{19/3}$	12	9
$8/3$	0	2
$\sqrt{8}$	24	18

We believe that tetrahedrally coordinated self-assembly via an isotropic potential is a counterintuitive result because conventional wisdom, based on atomic and molecular chemistry, has biased thinking toward the belief that highly anisotropic interactions are necessary for such locally directional structure as in diamond or wurtzite, as in the case of the carbon-carbon covalent bonds in the true diamond crystal. The present work constitutes a clear demonstration that this chemical intuition is too restrictive. We have previously found an isotropic potential that causes spontaneous assembly of the sixfold-coordinated simple cubic lattice [15], but the tetrahedral lattices present a significantly greater challenge. Finding such potentials is difficult, as the diamond and wurtzite lattices are close structural competitors with one another (and therefore close in energy for short-ranged potentials).

In order to understand how the diamond lattice is energetically distinguished from other lattices, consider wurtzite as a competitor to diamond in a system with an isotropic interaction potential. Whereas the diamond lattice can be considered as two interlaced fcc lattices, the wurtzite is two interlaced hexagonal close-packed (hcp) lattices. Both are tetrahedrally coordinated. For the sake of argument, call the nearest neighbor distance a in both lattices. Both have 12-fold-coordinated neighbors at $\sqrt{8/3}a \sim 1.63a$, but the wurtzite has a single extra neighbor at $(5/3)a$. Both have neighbors at $\sqrt{11/3}a$, but the diamond is 12-fold-coordinated there where the wurtzite is ninefold. It is evident that energetically differentiating between these two lattices (and causing one to self-assemble in a simulation rather than the other) using an isotropic, short-ranged potential is challenging. Table I gives the diamond and wurtzite coordination numbers for their first few coordination shells.

In Sec. II, we briefly discuss the optimization methodology, and then proceed in Sec. III to a discussion of the results for the diamond and wurtzite cases. In this section, we report on all necessary criteria: lattice sums, phonons, defect energies, and molecular dynamics (MD) self-assembly. We also include a discussion of the melting behavior of each crystal. We conclude in Sec. IV with some final comments about this approach.

II. METHODOLOGY

The inverse method used to obtain the interaction potentials $V_D(r)$ and $V_W(r)$ is discussed extensively in our previous work [16], and so will not be discussed here at any length. It is, however, important to note that this zero-temperature scheme optimizes the energetic stability of a given target lattice (in this case, diamond and wurtzite), in comparison to competitor lattices (chosen previously), subject to the condition that the target lattice is linearly mechanically stable at an appropriately chosen specific volume (inverse density). Linear stability is tested while the optimization is being carried out by calculating the phonon spectrum, and thus making sure that every normal mode of the crystal, at any given wave vector in the Brillouin zone (BZ), is real. The competitor lattices used were the fcc, bcc, hcp, simple hexagonal (hex), and simple cubic (sc) structures.

Of course the optimization scheme for the isotropic interaction cannot search over the entire space of functions of a single variable; therefore we choose a suitably normalized, well-motivated family of potentials defined by a finite number of parameters $\{a_0, \dots, a_n\}$, and find the set of a_i 's that maximizes the energetic difference between the target and competitor lattices subject to the constraint of linear mechanical stability at a particular specific volume.

III. RESULTS

A. Diamond

In this case, a parametrization was chosen such that the potential has three local minima, with the ratios of the positions of the second to the first and of the third to the first, being $\sqrt{8/3}$ and $\sqrt{11/3}$, respectively. These are the exact distance ratios of the neighbors in the diamond lattice. The target coordination numbers for the first three neighbors are 4, 12, and 12, and thus the first local minimum was constrained to be positive in the parametrization, in order to discriminate against close-packed and body-centered cubic lattices, which have coordination numbers 12 and 8, respectively. It should be noted that a number of different parametrizations were attempted, many with simpler functional forms (i.e., with fewer local minima and maxima), but the potential we report here is by all criteria the most suitable. It is

$$V_D(r) = \frac{5}{r^{12}} - \frac{6}{r^{10}} + 17.0 \exp(-2.5r) - 0.362477 \exp[-150 \times (r - 1.702)^2] - 0.263218 \exp[-166(r - 1.998)^2]. \quad (1)$$

This potential is shown in Fig. 1. It consists of a Lennard-Jones-type term (a 12–10 Lennard-Jones), an exponential decay, and two Gaussians that serve to localize the second and third neighbors for the sake of mechanical stability of the lattice. It is important to note here that this potential defines the energy and length units that we use for this study. Thus, derived quantities, such as pressure and volume, have units determined by the length and energy units of this potential.

In the optimization scheme, the specific volume is chosen for us: it is that which places the nearest neighbor of the

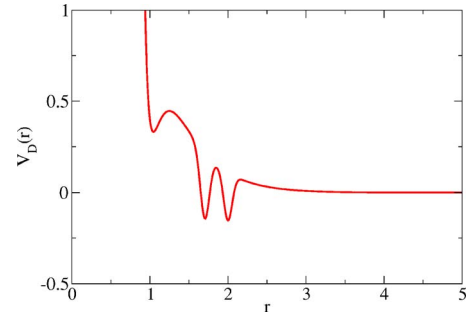


FIG. 1. (Color online) Functional form of the potential $V_D(r)$ given in Eq. (1). Given in reduced units.

diamond lattice exactly at the first local minimum. This occurs at $r=1.0450$, which sets the specific volume to be 1.756 94.

An essential ingredient of the optimization scheme is the lattice sums, which give the Madelung energies (crystal energies) of a number of lattices, including diamond, over a range of specific volume. These are shown in Fig. 2. Not only do the lattice sums show that the diamond lattice has the lowest energy of all of its competitors at the chosen v , but also the double-tangent construction yields the zero-temperature range of pressures in which the diamond lattice is stable. That range is 0.12 through 1.89, in terms of the units defined by the potential [Eq. (1)].

Fifteen molecular dynamics simulations (at constant number of particles, volume, and energy, microcanonically) were run in which 216 particles were started from a random configuration at $v=1.756 94$, at a temperature well above the freezing point (homogeneous case). Upon slow cooling, all simulations resulted in diamond lattices with differing numbers and types of defects, with 1 of 15 exhibiting no defects whatsoever. This configuration is shown in Fig. 3. Although it may not be immediately clear from the two-dimensional

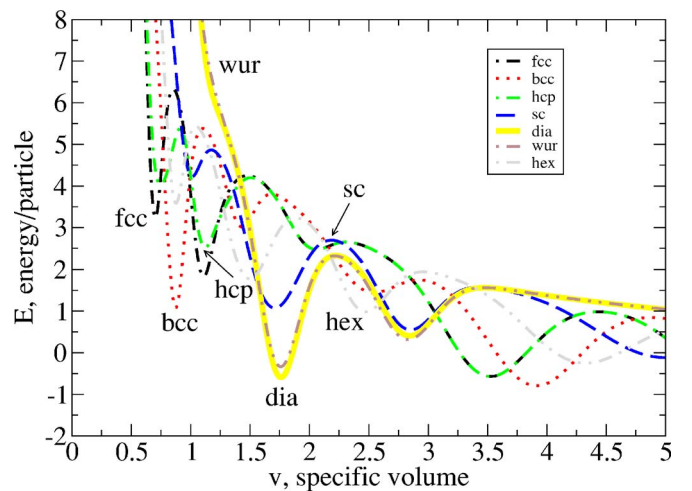


FIG. 2. (Color online) Lattice sums of seven lattices, including diamond, using the potential given in Eq. (1). The double-tangent construction determines that at zero temperature, the pressure range of stability for the diamond lattice is 0.12–1.89. Here, “dia” refers to diamond, “wur” to wurtzite, and “hex” to simple hexagonal (with $c/a=1$). Given in reduced units.

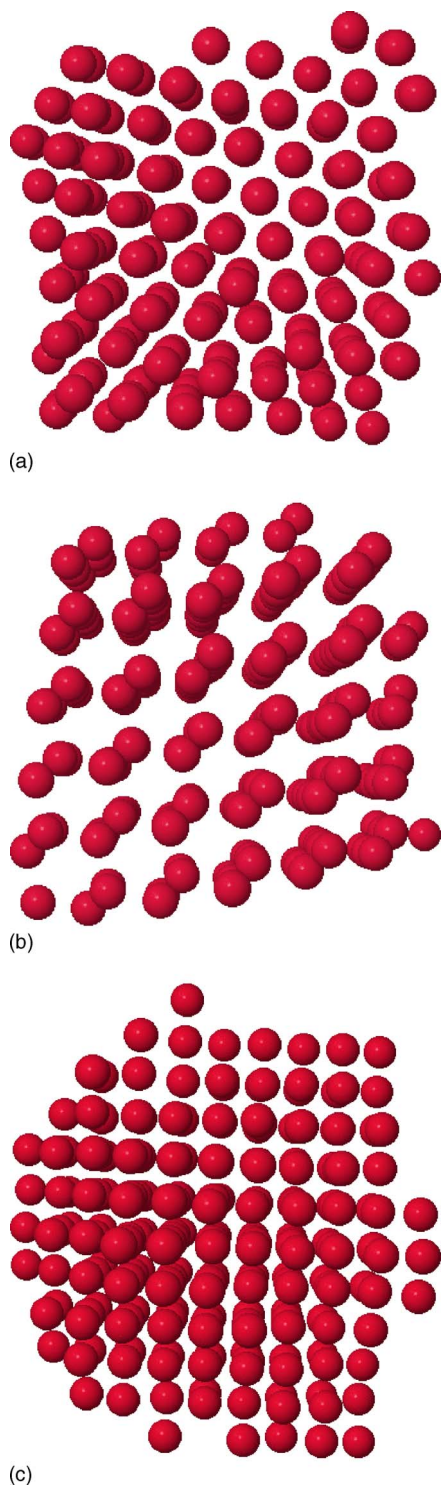


FIG. 3. (Color online) Results of MD simulation. 216 particles interacting via isotropic diamond potential $V_D(r)$ self-assemble into a perfect diamond configuration (one configuration shown from three different viewpoints is shown above). These three views clearly show that the result is the diamond lattice. Closer inspection of the configuration shows that it is indeed tetrahedrally coordinated. (a) View 1 shows triangular lattice slice of diamond. (b) View 2: “Hexagons” in this view are indicative of the diamond structure. (c) View 3: Square lattice shows most clearly the cubic symmetry of the diamond lattice.

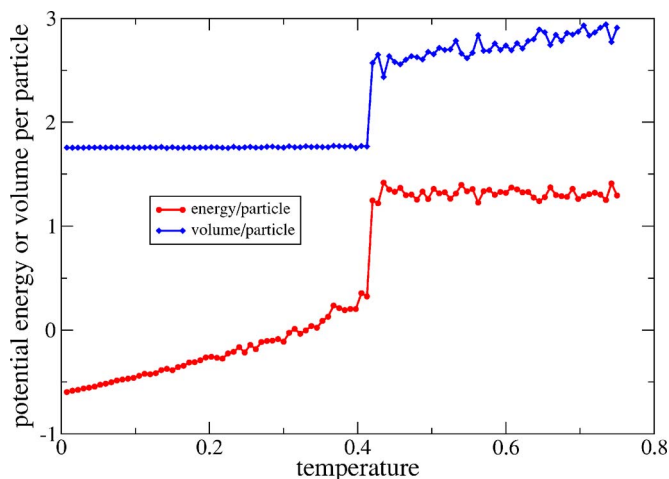


FIG. 4. (Color online) Volume per particle and potential energy per particle of the melting diamond crystal, as determined from a Monte Carlo simulation at fixed number of particles, pressure and temperature (NPT). The pressure here is 1.0, in units defined by Eq. (1). The volume curve (upper curve) shows that this system expands upon melting, unlike solid water (ice), which also has a tetrahedral structure. Note that the volume-per-particle curve indicates that the thermal expansion coefficient is virtually zero over the entire crystal stability range of temperatures. Clearly this melting transition is strongly first order. Given in reduced units.

projections, this is indeed the four-coordinated diamond lattice, with the first neighbor at distance $a=1.045$. The next neighbors are at $r_2=(\sqrt{8/3})a$ (12 coordinated), $r_3=(\sqrt{11/3})a$ (12 coordinated), and $r_4=(\sqrt{16/3})a$ (six coordinated), and so on. These are the correct distances and coordination numbers of the diamond lattice. Heterogeneous nucleation also produced self-assembly of the diamond lattice in a 252-particle system, with some point defects.

In order to calculate the energy of defects (vacancies and interstitials), molecular dynamics simulations were run in which a particle was either removed ($N=215$) or inserted ($N=217$). The diamond lattice is a sublattice of the bcc structure, and the interstitial was initially set on a nonoccupied bcc site (and it did not move significantly during the relaxation). The specific volume was set to be $v=1.75694$ in both cases. The vacancy energy was found to be 2.866 and the interstitial energy was 3.794.

In order to study the melting behavior of the crystal, Gibbs-ensemble Monte Carlo simulations were run (at constant number of particles, pressure, and temperature). The pressure was set to be 1.0, well within the range of stability of the lattice. The temperature in the simulation was slowly raised, starting near absolute zero, giving the system sufficient time to equilibrate, and the resulting volume and configurational energy recorded. These two quantities, plotted in Fig. 4, show a dramatic first-order melting transition. It is striking how flat is the volume-per-particle curve as a function of temperature, i.e., the thermal expansion coefficient is virtually zero over the entire crystal stability range of temperatures: a materials characteristic of important technological relevance. Another interesting property shown in this figure is that the system expands upon melting the crystal (by

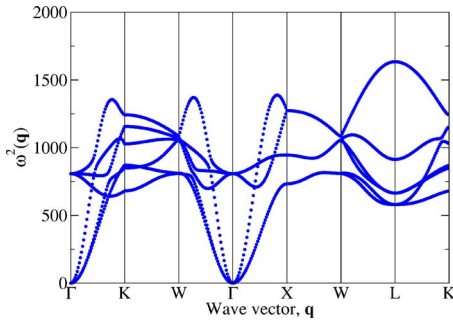


FIG. 5. (Color online) Phonon spectrum for the diamond lattice in which particles interact via $V_D(r)$, at specific volume $v = 1.75694$. Only certain trajectories between points of high symmetry in the Brillouin zone are shown, although at every wave vector $\omega^2(\mathbf{q}) \geq 0$. This implies that the crystal is linearly mechanically stable. Given in reduced units.

roughly 45%). This sort of qualitative behavior is what we would expect for a dense crystal, but perhaps not for such an open lattice as diamond. Indeed, solid water (ice) has a tetrahedral structure (as do real diamond and silicon) and contracts on melting, by approximately 8.3% at atmospheric pressure [17]. While there is no intrinsic reason to believe that our model system should act similarly, it is interesting to observe how qualitatively different its melting behavior is.

The phonon spectra for the potential $V_D(r)$ with particles arranged in a diamond lattice are shown in Fig. 5. For the wave vectors included in the plot, all modes have real frequencies (i.e., are propagating). We mention that, although only certain special wave vectors are shown in the plot, at the given specific volume $v = 1.75694$, all frequencies in the three-dimensional BZ are real, and thus the crystal is linearly mechanically stable.

B. Wurtzite

The wurtzite potential, $V_W(r)$, is given by

$$\begin{aligned}
 V_W(r) = & \frac{5}{r^{12}} - \frac{6.6}{r^{10}} + 4.553 \exp(-0.6r^4) \\
 & - 0.80 \exp[-100(r - \sqrt{8/3})^2] \\
 & - 0.40 \exp[-100(r - \sqrt{11/3})^2] \\
 & - 0.40 \exp[-100(r - \sqrt{16/3})^2].
 \end{aligned} \quad (2)$$

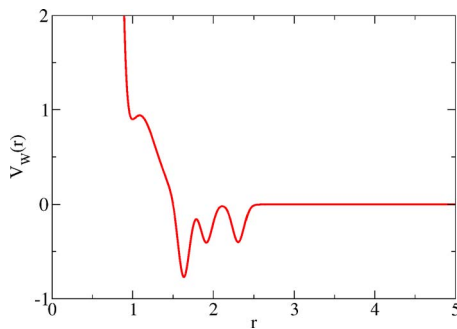


FIG. 6. (Color online) Functional form of the potential $V_W(r)$ given in Eq. (2). Given in reduced units.

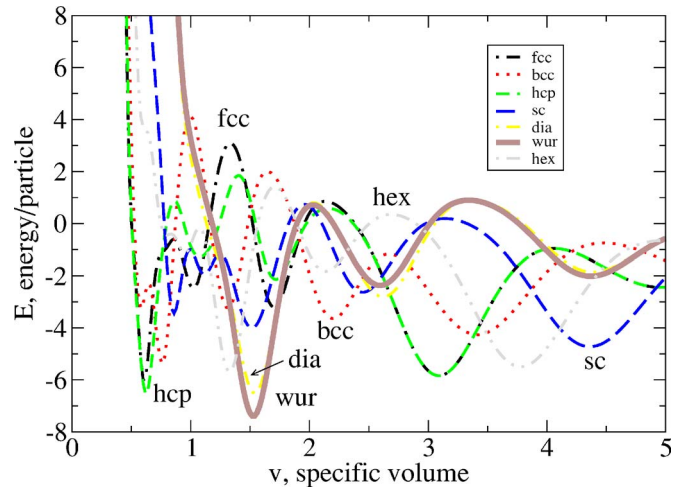


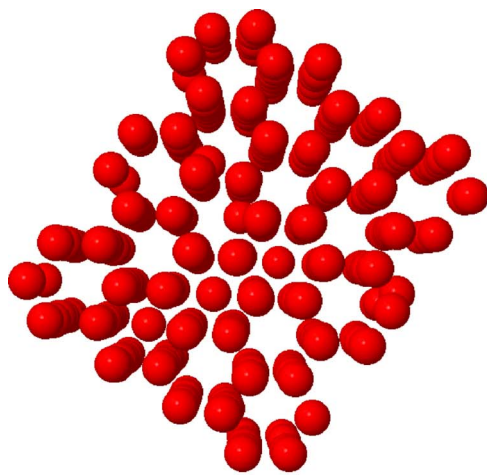
FIG. 7. (Color online) Lattice sums of seven lattices, including wurtzite, using the wurtzite potential V_W given in Eq. (2). The double-tangent construction determines that at zero temperature the pressure range of stability for the wurtzite lattice is 0.0–0.94. Given in reduced units.

This potential is shown in Fig. 6. The rationale for its shape is similar to that for diamond. The most important feature, perhaps, is the negative Gaussian centered at $\sqrt{16/3}$, because this is comparatively close to the next neighbor at $7/3$, which has sixfold coordination. The analogous neighbor in diamond is relatively separate from its next neighbor. For wurtzite, the specific volume is 1.539601.

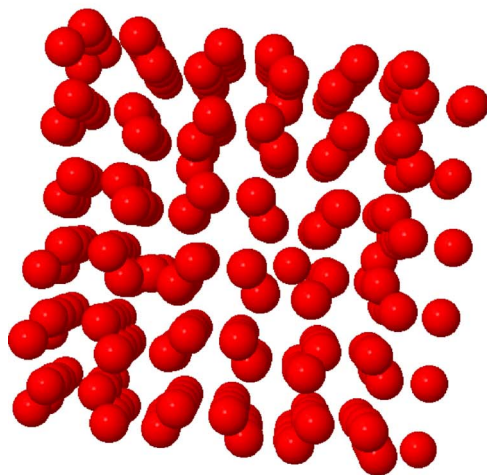
The lattice sums for $V_W(r)$ are given in Fig. 7. They show that there is a region of stability for the wurtzite lattice, and using the double-tangent construction, they give the pressure range of stability as from 0.0 through 0.94 in our reduced units. It is clear from the lattice sums that the hcp lattice is an important competitor to the wurtzite (at lower specific volume). This is natural: the wurtzite is nothing but two interlaced hcp lattices, just as the diamond is two interlaced fcc lattices.

The wurtzite crystal assembled upon heterogeneous, epitaxial growth from a fixed layer of particles within a 288-particle MD simulation, upon slow cooling. The layer consisted of two triangular lattice planes, one from each of the two interlaced hcp lattices, such that growth proceeded in the c direction (out of plane). All other particles in the system were inserted randomly. The self-assembly was not perfect, i.e., there were a number of (positive-energy) point defects remaining in the system that could not be annealed out, but this is to be expected for kinetic reasons.

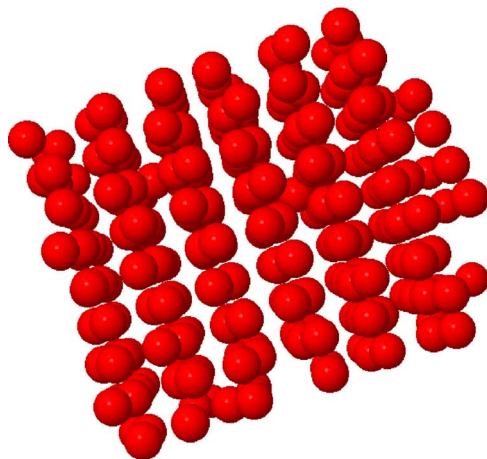
Defect calculations were performed as in Sec. III A, the diamond case. The vacancy energy was calculated by simply removing an atom from the perfect wurtzite crystal and allowing the system to relax in a microcanonical MD simulation (Fig. 8). We report the vacancy energy as 2.951, in reduced units. For the interstitial case, consider one of the two interlaced hcp lattices that together form wurtzite. This is an $ABAB\dots$ stacking of planar triangular lattices, contrasting with the $ABCABC\dots$ stacking of planar triangular lattices in the fcc structure. The wurtzite interstitial particle is placed in a triangular plane directly below the would-be C site. Its energy is reported as 8.889 in reduced units.



(a)



(b)



(c)

FIG. 8. (Color online) Results of MD simulation. 288 particles interacting via isotropic wurtzite potential $V_W(r)$ heterogeneously self-assemble into a near-perfect wurtzite configuration (one configuration is shown from three different viewpoints above). These three views clearly show that the result is the wurtzite lattice. Closer inspection of the configuration shows that it is indeed tetrahedrally coordinated. (a) View 1: Slice of wurtzite in which its characteristic hexagons are apparent. (b) View 2: Zigzags, also characteristic of wurtzite. (c) View 3: Another perspective.

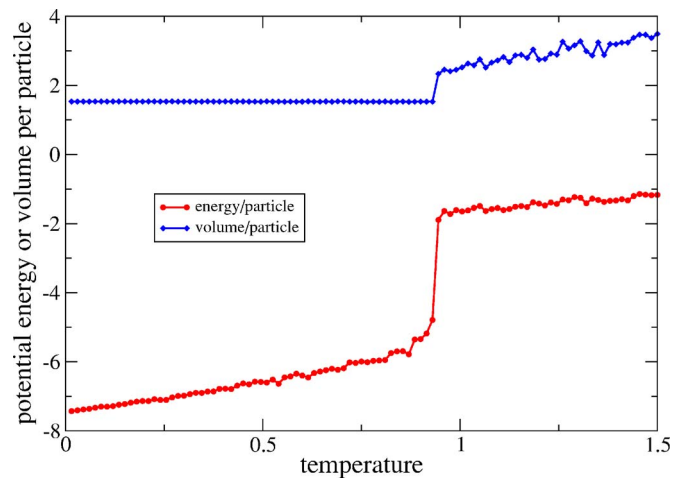


FIG. 9. (Color online) Volume per particle and potential energy per particle of the melting wurtzite crystal, as determined from an *NPT* Monte Carlo simulation. The pressure here is 0.5, in units defined by Eq. (1). The volume curve (upper) shows that this system expands upon melting, unlike solid water (ice), which also has a tetrahedral structure. As in the diamond case, the volume-per-particle curve indicates that the thermal expansion coefficient is virtually zero over the entire crystal stability range of temperatures. Clearly this melting transition is strongly first-order. Given in reduced units.

The melting behavior of the crystal was studied in the same way as that of the diamond crystal in the previous section was studied, namely, using Gibbs-ensemble Monte Carlo simulations. The pressure was set to be 0.5, well within the range of stability of the lattice. As in the diamond case, the temperature in the simulation was slowly raised, giving the system sufficient time to equilibrate, and the resulting volume and configurational energy recorded. These two quantities, plotted in Fig. 9, show dramatically how strongly first-order the melting transition is for the wurtzite case (expansion of roughly 50%). As in the diamond instance, the volume-per-particle curve as a function of temperature is strikingly flat, i.e., the thermal expansions are virtually zero over the entire crystal stability range of tem-

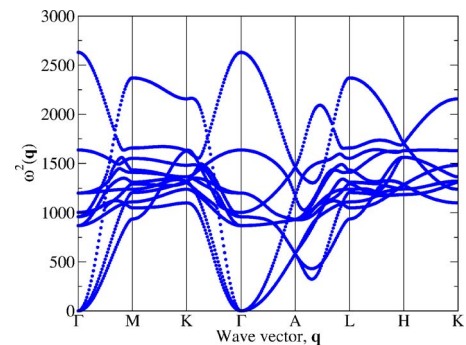


FIG. 10. (Color online) Phonon spectrum for the wurtzite lattice in which particles interact via $V_W(r)$ at specific volume $v = 1.539 601$. Only certain trajectories between points of high symmetry in the Brillouin zone are shown, although at every wave vector $\omega^2(\mathbf{q}) \geq 0$. This implies that the crystal is linearly mechanically stable. Given in reduced units.

peratures. The melting behavior is similar to the diamond case. It should be noted that this is qualitatively different from the behavior of ice-*Ih*, also a wurtzite structure, which contracts upon melting.

The wurtzite phonon spectrum is shown in Fig. 10. Trajectories of high symmetry are shown in the figure, but indeed all normal mode frequencies in the Brillouin zone are real, indicating that the crystal is linearly mechanically stable.

IV. CONCLUSIONS

In this paper, we have reported two isotropic interaction potentials such that in an N -body classical system with particles interacting via these potentials, the diamond and wurtzite lattices self-assemble as the system is slowly cooled. The functional forms of $V_D(r)$ and $V_W(r)$ were derived using an inverse statistical-mechanical methodology developed by the

authors, to be employed in tailoring intercomponent interactions to achieve self-assembly of targeted structures. Admittedly, these potentials have substantial radial complexity, but this is reminiscent of the complexity one sees in potentials of mean force in many-body systems. Furthermore, the possibilities of engineering multifeature potentials are growing significantly as the techniques of DNA and polymer functionalization of colloids and nanoparticles are refined. In future work, we plan on further exploring the self-assembly possibilities for isotropic potentials, including other carbon structures such as graphite, fullerenes, and nanotubes.

ACKNOWLEDGMENTS

We would like to kindly thank Christos Likos for very helpful and productive discussions during his visit to Princeton. This work was supported by the Office of Basic Energy Sciences, DOE, under Grant No. DE-FG02-04ER46108.

-
- [1] G. M. Whitesides, J. Mathias, and C. Seto, *Science* **254**, 5036 (1991).
 - [2] S. A. Jenekhe and X. L. Chen, *Science* **283**, 372 (1999).
 - [3] M.-P. Valignat, O. Theodoly, J. C. Crocker, W. B. Russel, and P. M. Chaikin, *Proc. Natl. Acad. Sci. U.S.A.* **102**, 4225 (2005).
 - [4] A. M. Jackson, J. W. Myerson, and F. Stellacci, *Nat. Mater.* **3**, 330 (2004).
 - [5] P. Mansky, C. K. Harrison, P. M. Chaikin, R. A. Register, and N. Yao, *Appl. Phys. Lett.* **68**, 2586 (1996).
 - [6] E. Rabani, D. R. Reichman, P. L. Geissler, and L. E. Brus, *Nature (London)* **426**, 271 (2003).
 - [7] K. M. Ho, C. T. Chan, and C. M. Soukoulis, *Phys. Rev. Lett.* **65**, 3152 (1990).
 - [8] M. C. Rechtsman, F. H. Stillinger, and S. Torquato, *Phys. Rev. Lett.* **95**, 228301 (2005).
 - [9] Z. L. Zhang, M. A. Horsch, M. H. Lamm, and S. C. Glotzer, *Nano Lett.* **3**, 1341 (2004).
 - [10] Y. Xia, B. Gates, and Z.-Y. Li, *Adv. Mater. (Weinheim, Ger.)* **13**, 409 (2001).
 - [11] W. Man, M. Megens, P. Steinhardt, and P. Chaikin, *Nature (London)* **436**, 993 (2005).
 - [12] B. Montgomery Pettitt and M. Karplus, *Chem. Phys. Lett.* **121**, 194 (1985).
 - [13] A. M. Kalsin, M. Fialkowski, M. Paszewski, S. K. Smoukov, K. J. M. Bishop, and B. A. Grzybowski, *Science* **312**, 420 (2006).
 - [14] M. Watzlawek, C. N. Likos, and H. Lowen, *Phys. Rev. Lett.* **82**, 5289 (1999).
 - [15] M. C. Rechtsman, F. H. Stillinger, and S. Torquato, *Phys. Rev. E* **74**, 021404 (2006).
 - [16] M. Rechtsman, F. Stillinger, and S. Torquato, *Phys. Rev. E* **73**, 011406 (2006).
 - [17] D. Eisenberg and W. Kauzmann, *The Structure and Properties of Water* (Oxford University Press, London, 1969).